Numerical modeling of neutron transport in SP_3 approximation by finite element method

Alexander V. Avvakumov[a], Valery F. Strizhov[b], Petr N. Vabishchevich[b,c,*], Alexander O. Vasilev[c]

[a] *National Research Center* Kurchatov Institute*, 1, Sq. Academician Kurchatov, Moscow, Russia*
[b] *Nuclear Safety Institute, Russian Academy of Sciences, 52, B. Tulskaya, Moscow, Russia*
[c] *North-Eastern Federal University, 58, Belinskogo, Yakutsk, Russia*

Abstract

The SP_3 approximation of the neutron transport equation allows improving the accuracy for both static and transient simulations for reactor core analysis compared with the neutron diffusion theory. Besides, the SP_3 calculation costs are much less than higher order transport methods (S_N or P_N). Another advantage of the SP_3 approximation is a similar structure of equations that is used in the diffusion method. Therefore, there is no difficulty to implement the SP_3 solution option to the multi-group neutron diffusion codes. In this work, the application of the SP_3 methodology based on solution of the λ- and α-spectral problems has been tested for the IAEA-2D and HWR reactor benchmark tests. The FEM is chosen to achieve the 3D geometrical generality, using GMSH as a generic mesh generator. The results calculated with the diffusion and SP_3 methods are compared with the reference transport calculation results. It was found for the HWR reactor test that some eigenvalues are complex when calculating using both diffusion and SP_3 options.

Keywords: neutron transport equation, diffusion theory, SP_3 approximation, reactor core, spectral problems, eigenvalues.

1. Introduction

The diffusion approximation of the neutron transport equation is widely used in nuclear reactor analysis allowing whole-core calculations with reasonable accuracy. The main feature of neutron diffusion equation is following: it is assumed that the neutron current is proportional to the neutron flux gradient (the Ficks law). There are also three assumptions: neutron absorption much less

*Corresponding author
Email addresses: Avvakumov2009@rambler.ru (Alexander V. Avvakumov), vfs@ibrae.ac.ru (Valery F. Strizhov), vabishchevich@gmail.com (Petr N. Vabishchevich), haska87@gmail.com (Alexander O. Vasilev)

likely than scattering, linear spatial variation of the neutron distribution and isotropic scattering (Stacey, 2007). To provide the validity of diffusion theory, the modern diffusion codes use, as a rule, assembly-by-assembly coarse-mesh calculation scheme with effective homogenized cross sections, prepared by more accurate transport approximations. To improve the diffusion code restrictions related with limitations on mesh spacing, different approaches are used including nodal and finite element methods (Avvakumov et al., 2017; Lawrence, 1986).

For many situations of interest (for instance, the pin-by-pin calculation taking account strongly absorbing control rods), the applicability of neutron diffusion theory are limited. Therefore, a more rigorous approximation for the neutron transport is required.

The solution of the neutron transport equation is very complicated problem because of seven independent variables: five for space-angular description, one for energy and one for time. To simplify the transport problem, different approaches are used such as the spherical harmonics (P_N) approximation (Azmy and Sartori, 2010). The P_N approximation of the neutron transport equation is derived by expansion of the angular dependence of the neutron flux in the N spherical harmonics. During the last time, the simplest version of the P_N method, namely the simplified P_N approximation became widespread (McClarren, 2010). The major feature of the SP_N method is following: the three-dimensional neutron transport equation is transformed to a set of one-dimensional equations. The number of the SP_N trial functions is equal to $2(N+1)$ compared with the P_N method which uses $(N+1)^2$ trial functions. This leads to significant reduce in the computation time for typical whole-core calculations.

The SP_N approximation was first derived by Gelbard (Gelbard, 1960, 1961, 1962) in the early 1960s. He replaced the spatial derivatives with Laplacian and divergence operators in a one-dimensional planar geometry. The resulting SP_N equations are elliptic, for example, the SP_3 equations consist of two equations of diffusion type with two unknown fluxes: the scalar flux and the second angular flux moment. More rigorous theoretical foundation of the SP_3 methodology has been derived by Brantley and Larsen (Brantley and Larsen, 2000) on the basis of variational methods.

The SP_3 method, as expected, can provide accuracy improvement compared with the common used diffusion method. Besides, implementation of the SP_3 equations into the diffusion code is not difficult because of the similar structure of the SP_3 and diffusion equations. For this reason the SP_3 method was adopted in different whole-core calculation codes, such as DYN3D (Beckert and Grundmann, 2008), PARCS (Downar et al., 2010) and others. According to (Tada et al., 2008), application of the SP_3 theory to the pin-by-pin calculation for BWR geometry resulted in remarkable improvement in the calculation accuracy compared with the diffusion method. Another report (Brewster, 2018) shows the comparison of the diffusion and SP_3 methods to calculate the control rod reactivity in a light-water reactor. As compared with the Monte Carlo reference calculation, the SP_3 method gives twice as accurate result compared with the diffusion method. Besides, as it turned out, the computation time using the

SP_3 method is only 1.5 times longer than that using the diffusion method (Tada et al., 2008).

Thus, the SP_3 method can be considered as an improved approximation of the neutron transport equation compared with the diffusion method. In this regard, it will be very useful to compare the spectral parameters, calculated by both the diffusion and SP_3 methods. To characterize the reactor steady-state conditions or dynamic behavior, some spectral problems are considered (Stacey, 2007; Bell and Glasstone, 1970). The steady-state condition is usually described by solution of a spectral problem (λ-eigenvalue problem); the fundamental eigenvalue (the largest eigenvalue) is called k-effective of the reactor core (Stacey, 2007; Bell and Glasstone, 1970). The reactor dynamic behavior can naturally be described on the basis of the approximate solution expansion in time-eigenvalue of α-eigenvalue problem (Ginestar et al., 2002; Verdu et al., 2010; Verdu and Ginestar, 2014). At large times, one can talk about the asymptotic behavior of a neutron flux, whose amplitude is $\exp(\alpha t)$. Previously the complex eigenvalues and eigenfunctions were found in the spectral problems for some numerical tests (Avvakumov et al., 2017).

In this paper we consider the SP_3 approximation for the steady-state multigroup neutron transport problem. To solve spectral problems with nonsymmetrical matrices we use well-designed algorithms and relevant free software including the library SLEPc (Scalable Library for Eigenvalue Problem Computations, http://slepc.upv.es/). We use a Krylov-Schur algorithm, a variation of Arnoldi method, described in (Stewart, 2001).

The paper is organized as follows. The steady-state and dynamic models of a nuclear reactor based on the multigroup SP_3 equations are given in Section 2. In Section 3 we discuss various spectral problems. Some numerical examples of calculation of spectral characteristics of two-dimensional test problems for IAEA-2D benchmark problem and HWR reactor using the two-group system of diffusion and SP_3 equations is discussed in Section 4. The results of the work are summarized in Section 5.

2. Problem statement

Lets consider the symmetric form of the SP_3 equation for the neutron flux (Ryu and Joo, 2013). The neutron dynamics is considered in the limited convex two-dimensional or three-dimensional area Ω ($\boldsymbol{x} = \{x_1, ..., x_d\} \in \Omega,\ d = 2, 3$) with boundary $\partial\Omega$. The neutron transport is described by the system of equations

$$\begin{aligned}
&\frac{1}{v_g}\frac{\partial\phi_{0,g}}{\partial t} - \frac{2}{v_g}\frac{\partial\phi_{2,g}}{\partial t} - \nabla\cdot D_{0,g}\nabla\phi_{0,g} + \Sigma_{r,g}\phi_{0,g} - 2\Sigma_{r,g}\phi_{2,g} = \\
&\qquad = (1-\beta)\chi_{n,g}S_n + S_{s,g} + \chi_{d,g}S_d, \\
&-\frac{2}{v_g}\frac{\partial\phi_{0,g}}{\partial t} + \frac{9}{v_g}\frac{\partial\phi_{2,g}}{\partial t} - \nabla\cdot D_{2,g}\nabla\phi_{2,g} + (5\Sigma_{t,g} + 4\Sigma_{r,g})\phi_{2,g} - 2\Sigma_{r,g}\phi_{0,g} = \\
&\qquad = -2(1-\beta)\chi_{n,g}S_n - 2S_{s,g} - 2\chi_{d,g}S_d,
\end{aligned} \tag{1}$$

where

$$S_n = \sum_{g'=1}^{G} \nu\Sigma_{f,g'}\phi_{g'}, \quad S_{s,g} = \sum_{g\neq g'=1}^{G} \Sigma_{s,g'\to g}\phi_{g'}, \quad S_d = \sum_{m=1}^{M} \lambda_m c_m,$$

$$\phi_{0,g} = \phi_g + 2\phi_{2,g}, \quad D_{0,g} = \frac{1}{3\Sigma_{tr,g}}, \quad D_{2,g} = \frac{9}{7\Sigma_{t,g}}, \quad g = 1, 2, ..., G.$$

Here G — number of energy groups, $\phi_g(\boldsymbol{x}, t)$ — scalar flux, $\phi_{0,g}(\boldsymbol{x}, t)$ — pseudo 0th moment of angular flux, $\phi_{2,g}(\boldsymbol{x}, t)$ — second moment of angular flux, $\Sigma_{t,g}(\boldsymbol{x}, t)$ — total cross-section, $\Sigma_{tr,g}(\boldsymbol{x}, t)$ — transport cross-section, $\Sigma_{r,g}(\boldsymbol{x}, t)$ — removal cross-section, $\Sigma_{s,g'\to g}(\boldsymbol{x}, t)$ — scattering cross-section, χ_g — spectra of neutrons, $\nu\Sigma_{f,g}(\boldsymbol{x}, t)$ — generation cross-section, $c_m(\boldsymbol{x}, t)$ — density of sources of delayed neutrons, λ_m — decay constant of sources of delayed neutrons, M — number of types of delayed neutrons.

The density of sources of delayed neutrons is described by the equations

$$\frac{\partial c_m}{\partial t} + \lambda_m c_m = \beta_m S_n, \quad m = 1, 2, ..., M, \tag{2}$$

where β_m is the fraction of delayed neutrons of m-type, and

$$\beta = \sum_{m=1}^{M} \beta_m.$$

The Marshak-type conditions are set at the boundary of the area $\partial\Omega$

$$\begin{bmatrix} J_{0,g}(\boldsymbol{x}) \\ J_{2,g}(\boldsymbol{x}) \end{bmatrix} = \begin{bmatrix} \frac{1}{2} & -\frac{3}{8} \\ -\frac{3}{8} & \frac{21}{8} \end{bmatrix} \begin{bmatrix} \phi_{0,g}(\boldsymbol{x}) \\ \phi_{2,g}(\boldsymbol{x}) \end{bmatrix}, \quad J_{i,g}(\boldsymbol{x}) = -D_{i,g}\nabla\phi_{i,g}(\boldsymbol{x}), \quad i = 0, 2. \tag{3}$$

System of equations (1) and (2) is supplemented with boundary conditions (3) and corresponding initial conditions

$$\phi_g(\boldsymbol{x}, 0) = \phi_g^0(\boldsymbol{x}), \quad g = 1, 2, ..., G, \quad c_m(\boldsymbol{x}, 0) = c_m^0(\boldsymbol{x}), \quad m = 1, 2, ..., M. \tag{4}$$

Let's write the boundary problem (1)–(4) in operator form. The vectors $\boldsymbol{u}_1 = \{\phi_{0,1}, \phi_{0,2}, \cdots, \phi_{0,G}\}$, $\boldsymbol{u}_2 = \{\phi_{2,1}, \phi_{2,2}, \cdots, \phi_{2,G}\}$, $\boldsymbol{c} = \{c_1, c_2, ..., c_M\}$ and matrices are defined as follows

$$V = (\mathrm{v}_{gg'}), \ \mathrm{v}_{gg'} = \frac{1}{v_g}\delta_{gg'}, \quad B = (b_{gg'}), \ b_{gg} = -2\Sigma_{r,g}, \ b_{gg'} = 2\Sigma_{s,g'\to g},$$

$$A_1 = (a_{gg'}), \ a_{gg} = -\nabla\cdot D_{0,g}\nabla + \Sigma_{r,g}, \ a_{gg'} = -\Sigma_{s,g'\to g},$$
$$A_2 = (a_{gg'}), \ a_{gg} = -\nabla\cdot D_{2,g}\nabla + 5\Sigma_{tr,g} + 4\Sigma_{r,g}, \ a_{gg'} = -4\Sigma_{s,g'\to g},$$
$$F = (f_{gg'}), \ f_{gg'} = \chi_{n,g}\nu\Sigma_{f,g'}, \quad E = (e_{gm}), \ e_{gm} = \chi_{d,g}\lambda_m,$$

$$\Lambda = (\lambda_{mm'}),\ \ \lambda_{mm'} = \delta_{mm'}\lambda_m, \quad Q = (q_{mg}),\ \ q_{mg} = \beta_m \nu \Sigma_{f,g},$$

where

$$\delta_{gg'} = \begin{cases} 1, & g = g', \\ 0, & g \neq g', \end{cases}$$

is the Kronecker symbol. We shall use the set of vectors $\boldsymbol{u}$, whose components satisfy the boundary conditions (3). Using the set definitions, the system of equations (1) and (2) can be written as following

$$\begin{gathered} V(\frac{\partial \boldsymbol{u}_1}{\partial t} - 2\frac{\partial \boldsymbol{u}_2}{\partial t}) + A_1\boldsymbol{u}_1 + B\boldsymbol{u}_2 = (1-\beta)F(\boldsymbol{u}_1 - 2\boldsymbol{u}_2) + E\boldsymbol{c}, \\ V(-2\frac{\partial \boldsymbol{u}_1}{\partial t} + 9\frac{\partial \boldsymbol{u}_2}{\partial t}) + A_2\boldsymbol{u}_2 + B\boldsymbol{u}_1 = -2(1-\beta)F(\boldsymbol{u}_1 - 2\boldsymbol{u}_2) - 2E\boldsymbol{c}, \\ \frac{\partial \boldsymbol{c}}{dt} + \Lambda\boldsymbol{c} = Q(\boldsymbol{u}_1 - 2\boldsymbol{u}_2). \end{gathered} \tag{5}$$

Without taking into account delayed neutrons (all neutrons are considered as prompt), we have

$$\begin{gathered} V(\frac{\partial \boldsymbol{u}_1}{\partial t} - 2\frac{\partial \boldsymbol{u}_2}{\partial t}) + A_1\boldsymbol{u}_1 + B\boldsymbol{u}_2 = F(\boldsymbol{u}_1 - 2\boldsymbol{u}_2), \\ V(-2\frac{\partial \boldsymbol{u}_1}{\partial t} + 9\frac{\partial \boldsymbol{u}_2}{\partial t}) + A_2\boldsymbol{u}_2 + B\boldsymbol{u}_1 = -2F(\boldsymbol{u}_1 - 2\boldsymbol{u}_2). \end{gathered} \tag{6}$$

The Cauchy problem is formulated for equations (5) and (6) when

$$\boldsymbol{u}_1(0) = \boldsymbol{u}_1^0, \quad \boldsymbol{u}_2(0) = \boldsymbol{u}_2^0, \quad \boldsymbol{c}(0) = \boldsymbol{c}^0, \tag{7}$$

where $\boldsymbol{u}_1^0 = \{\phi_{0,1}^0, \phi_{0,2}^0, ..., \phi_{0,G}^0\}$, $\boldsymbol{u}_2^0 = \{\phi_{2,1}^0, \phi_{2,2}^0, ..., \phi_{2,G}^0\}$ and $\boldsymbol{c}^0 = \{c_1^0, c_2^0, ..., c_M^0\}$.

3. Spectral problems

To characterize the reactor dynamic processes described by Cauchy problem (5)-(7), lets consider some spectral problems (Bell and Glasstone, 1970; Stacey, 2007).

The spectral problem, which is known as the λ-spectral problem, is usually considered. For the system of equations (6), (7), we have

$$L\boldsymbol{\varphi} = \lambda^{(k)} M\boldsymbol{\varphi}, \tag{8}$$

where

$$\boldsymbol{\varphi} = \{\boldsymbol{\varphi}_1, \boldsymbol{\varphi}_2\}, \quad L = \begin{pmatrix} A_1 & B \\ B & A_2 \end{pmatrix}, \quad M = \begin{pmatrix} F & -2F \\ -2F & 4F \end{pmatrix}.$$

The minimal eigenvalue is used for characterisation of neutron field, thus

$$k = \frac{1}{\lambda_1^{(k)}}$$

is the effective multiplication factor (k-effective). The value $k = \lambda_1^{(k)} = 1$ is related to the critical state of the reactor, and the corresponding eigenfunction $\boldsymbol{\varphi}^{(1)}(\boldsymbol{x})$ is the stationary solution of the Eq (5), (6). At $k > 1$, one can speak about supercriticality, at $k < 1$ — about subcriticality.

The spectral problem (8) cannot directly be connected with the dynamic processes in a nuclear reactor. The eigenvalues of the multiplication factor of the reactor and the corresponding eigenfunctions do not depend on the time delay for the emission of delayed neutrons. The reason is that the problem (8) on eigenvalues is the problem of finding time-independent solutions of the neutron transport equation, and the term describing the contribution of fission to the neutron balance is equal to the total number of fission neutrons, both instantaneous and delayed divided by k. At the best, we can get only the limiting case — the stationary critical state. The more acceptable spectral characteristics for the non-stationary equation (5) are related the spectral problem

$$\begin{gathered} L\boldsymbol{\varphi} - (1-\beta)M\boldsymbol{\varphi} - I\boldsymbol{s} = \lambda^{(\alpha)} W\boldsymbol{\varphi}, \\ \Lambda\boldsymbol{s} - R\boldsymbol{\varphi} = \lambda^{(\alpha)}\boldsymbol{s}. \end{gathered} \tag{9}$$

The α-eigenvalue problem without delayed neutrons (6) can be written as follows

$$L\boldsymbol{\varphi} - M\boldsymbol{\varphi} = \lambda^{(\alpha)} W\boldsymbol{\varphi}, \tag{10}$$

where

$$I = \begin{pmatrix} E \\ -2E \end{pmatrix}, \quad R = \begin{pmatrix} Q & -2Q \end{pmatrix}, \quad W = \begin{pmatrix} V & -2V \\ -2V & 9V \end{pmatrix}$$

The fundamental eigenvalue

$$\alpha = \lambda_1^{(\alpha)}$$

is called (Bell and Glasstone, 1970) the α-eigenvalue or the period eigenvalue, because it is inversely related to the reactor period. The problem of the period eigenvalues essentially takes into account the contribution of delayed neutrons. In particular, the long lifetime of the predecessors of delayed neutrons makes a large contribution to the slowly decreasing eigenfunctions of the reactor period, and this does not occur when only instantaneous neutrons are taken into account.

The asymptotic behaviour of Cauchy problem solution (5)-(7) at large times can be connected with the eigenvalue α. In this regular mode, the reactor behaviour is described by the function $\exp(-\alpha t)\boldsymbol{\varphi}^{(1)}(\boldsymbol{x})$. If $\alpha = 0$, then the reactor is critical; if $\alpha > 0$, then we get the neutron flux decreasing (subcritical state), and if $\alpha < 0$, then we get the neutron flux increasing (supercritical state).

There is a simple approximate relationship between the dominant eigenvalues of the k- and α-spectral problems without delayed neutrons:

$$\frac{1-k}{k} \approx \alpha\,\Lambda_{pr},\ 1-k \approx \alpha\, l_{pr}, \tag{11}$$

where Λ_{pr} — the prompt neutron generation time and l_{pr} — the prompt neutron lifetime.

4. Numerical examples

To study the properties of the eigenvalues and eigenfunctions of dufferent types, several benchmarks are studied. The first benchmark is the IAEA-2D two dimensional hexagonal problem of VVER-type without reflector (Chao and Shatilla, 1995). The second benchmark is the similar test but with radial reflector (Chao and Shatilla, 1995). The aim of the third test is to investigate azimutally non-symmetric effects on the eigenvalues and eigenfunctions (the changed IAEA-2D test with reflector). Finally, we studied the complex eigenvalues and eigenfunctions for the heavy water hexagonal reactor test HWR (Chao and Shatilla, 1995).

The two-group model ($G = 2$) is used in all tests. The method of finite elements (Brenner and Scott, 2008; Quarteroni and Valli, 2008) on triangular calculation grids is used for the approximate solution of the spectral problem. The standard Lagrangian finite elements are used. The software has been developed using the engineering and scientific calculation library FEniCS (Logg et al., 2012). SLEPc has been used for numerical solution of the spectral problems. We used a Krylov-Schur algorithm with an accuracy of 10^{-15}. The following parameters were varied in the calculations:

- n — the number of triangles per one assembly (Fig. 1);
- p — the order of finite element.

In this work we compare the SP_3 calculations with the previous diffusion model calculations (Avvakumov et al., 2014, 2017).

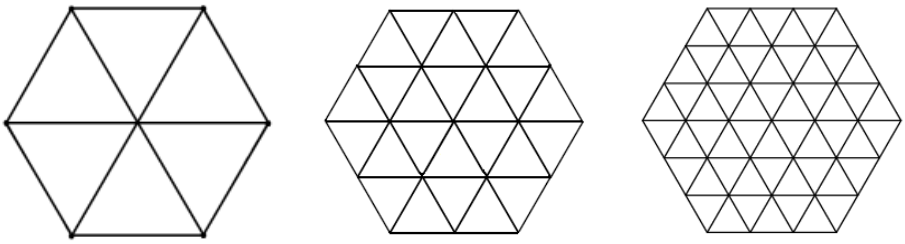

Figure 1: Discretization of assembly into 6, 24 and 96 finite elements.

4.1. IAEA-2D without reflector

The geometrical model of the IAEA-2D reactor core (Chao and Shatilla, 1995) consists of a set of hexagonal assemblies and is presented in Fig. 2, where the assemblies of various types are marked with various digits. The total size of assembly equals 20 cm.

Diffusion neutronics constants in the common units are given in Table 1. The following delayed neutrons parameters are used: one group of delayed neutrons with effective fraction $\beta_1 = 6.5{\cdot}10^{-3}$ and decay constant $\lambda_1 = 0.08\ \mathrm{s}^{-1}$. Neutron velocity $v_1 = 1.25 \cdot 10^7$ cm/s and $v_2 = 2.5 \cdot 10^5$ cm/s.

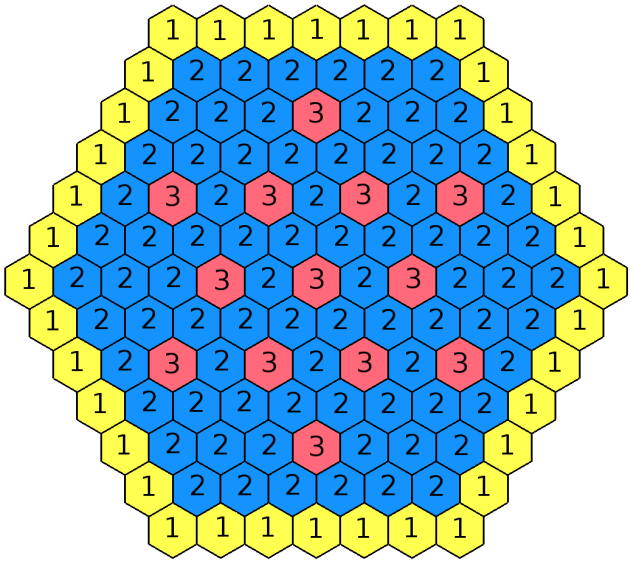

Figure 2: Geometrcial model of the IAEA-2D reactor core without reflector.

4.1.1. Solution of Lambda Modes spectral problem

As a reference solution for the diffusion model, we used the previous results (Avvakumov et al., 2014); for the SP_3 model — the solution obtained using very fine mesh ($p = 3, n = 96$). The maximum difference in assembly power between two models is about 2 percent for the rodded assemblies (material 3, see Fig. 2).

The results of the solution of the effective multiplication factor for test IAEA-2D without a reflector are shown in Table 2. Hereinafter, for λ-spectral problems, the following notation is used: k_{dif} — effective multiplication factor for the diffusion model; k_{sp_3} — effective multiplication factor for the SP_3 model; Δ — absolute deviation from the reference value in pcm (10^{-5}); δ — the standard deviation of the relative power in percent. These data demonstrate the convergence of the computed eigenvalues with refinement of the calculation mesh and increase in polynomial degree.

The results of the first 10 eigenvalues for $p = 3, n = 96$ are shown in Table 3. The power and error distributions for the diffusion and SP_3 models are presented in Figs 3 and 4 for $p = 2, n = 24$. Hereinafter, for each assembly the following data are given: the reference solution (the diffusion or SP_3 model), the solution for $p = 2, n = 24$ and the relative error from the reference solution.

Table 1: Diffusion neutronics constants for IAEA-2D.

Material	1	2	3	4
D_1	1.5	1.5	1.5	1.5
D_2	0.4	0.4	0.4	0.4
Σ_{a1}	0.01	0.01	0.01	0.0
Σ_{a2}	0.08	0.085	0.13	0.01
$\Sigma_{s,1\to2}$	0.02	0.02	0.02	0.04
$\Sigma_{s,1\to1}$	0.1922222	0.1922222	0.1922222	0.1822222
$\Sigma_{s,2\to2}$	0.7533333	0.7483333	0.7033333	0.8233333
$\nu_1\Sigma_{f1}$	0.00	0.00	0.00	0.00
$\nu_2\Sigma_{f2}$	0.135	0.135	0.135	0.00

Table 2: The effective multiplication factor.

n	p	k_{dif}	Δ_{dif}, pcm	δ_{dif}	k_{sp_3}	Δ_{sp_3}, pcm	δ_{sp_3}
	1	0.97335	473	3.80	0.97445	490	4.02
6	2	0.97760	48	0.45	0.97881	54	0.52
	3	0.97801	7	0.07	0.97925	10	0.09
	1	0.97654	154	1.28	0.97772	163	1.38
24	2	0.97799	9	0.08	0.97923	12	0.11
	3	0.97807	1	0.01	0.97934	1	0.02
	1	0.97765	43	0.36	0.97888	47	0.40
96	2	0.97807	1	0.02	0.97933	2	0.02
	3	0.97808	0	0.01	0.97935	–	–
Ref.		0.97808			0.97935		

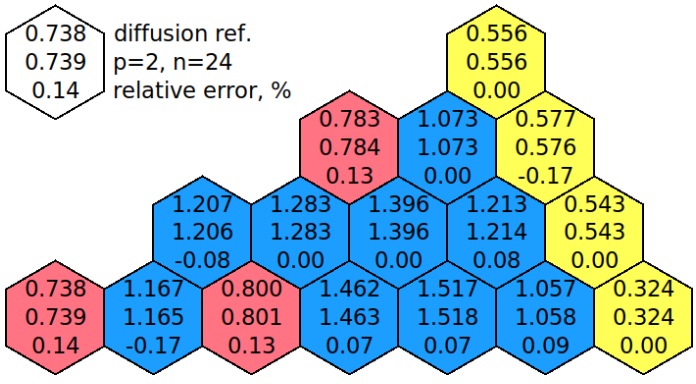

Figure 3: Power and error distributions using the diffusion model.

Table 3: The eigenvalues $k_i = 1/\lambda_i^{(k)}$ for $p = 3, n = 96$.

i	Diffusion	SP_3
1	$0.978076 + 0.0i$	$0.979351 + 0.0i$
2	$0.963180 + 0.0i$	$0.964604 + 0.0i$
3	$0.963180 + 0.0i$	$0.964604 + 0.0i$
4	$0.938438 + 0.0i$	$0.940253 + 0.0i$
5	$0.938438 + 0.0i$	$0.940253 + 0.0i$
6	$0.919658 + 0.0i$	$0.921844 + 0.0i$
7	$0.902198 + 0.0i$	$0.904467 + 0.0i$
8	$0.871410 + 0.0i$	$0.874997 + 0.0i$
9	$0.849566 + 0.0i$	$0.853155 + 0.0i$
10	$0.849565 + 0.0i$	$0.853154 + 0.0i$

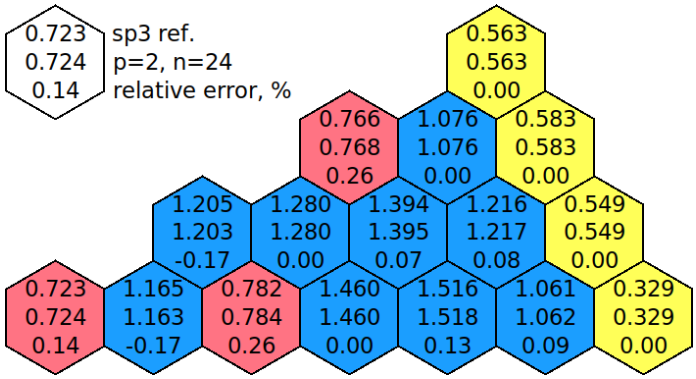

Figure 4: Power and error distributions using the SP_3 model.

4.1.2. Solution of α-spectral problem without delayed neutrons

As a reference solution for both the diffusion and transport SP_3 models, we used the solutions obtained using very fine mesh ($p = 3, n = 96$). Hereinafter, for α-spectral problems, the following notation is used: α_{dif} — α-eigenvalue by diffusion model; α_{sp_3} — α-eigenvalue by SP_3 model; Δ — absolute deviation from the reference value.

The calculation results for the α-spectral problem without delayed neutrons using the different meshes and the finite element orders are shown in Table 4. These data demonstrate the convergence of approximate computed eigenvalues with refinement of the calculation mesh and increase in polynomial degree.

According to (11), the prompt neutron lifetime $l_{pr} \approx 4.8 \cdot 10^{-5}$ sec for both the diffusion and SP_3 models at any mesh parameters.

The spectral problem results for the first 10 eigenvalues are shown in Table 5. The eigenvalues $\lambda_1^{(\alpha)} \leq \lambda_2^{(\alpha)} \leq ...$ are well separated. In this example,

Table 4: The α- eigenvalues.

n	p	α_{dif}	Δ_{dif}	α_{sp_3}	Δ_{sp_3}
6	1	556.3	100.8	532.7	104.1
	2	465.6	10.1	440.0	11.4
	3	457.0	1.5	430.7	2.1
24	1	488.1	32.6	463.0	34.4
	2	457.4	1.9	431.0	2.4
	3	455.7	0.2	428.9	0.3
96	1	464.6	9.1	438.4	9.8
	2	455.8	0.3	428.9	0.3
	3	455.5	–	428.6	–
Ref.		455.5		428.6	

the fundamental eigenvalue is less compared the rest and therefore the main harmonic will attenuate more slowly. A regular mode of the reactor is thereby defined. The value $\alpha = \lambda_1^{(\alpha)}$ determines the amplitude of neutron flux and is connected directly with reactor period in the regular mode.

Table 5: The eigenvalues $\alpha_i = \lambda_i^{(\alpha)}$ for $p = 3, n = 96$.

i	Diffusion	SP_3
1	$455.540 + 0.0i$	$428.561 + 0.0i$
2	$760.532 + 0.0i$	$730.398 + 0.0i$
3	$760.543 + 0.0i$	$730.408 + 0.0i$
4	$1267.192 + 0.0i$	$1228.835 + 0.0i$
5	$1267.192 + 0.0i$	$1228.836 + 0.0i$
6	$1647.145 + 0.0i$	$1601.437 + 0.0i$
7	$2083.289 + 0.0i$	$2031.778 + 0.0i$
8	$2696.887 + 0.0i$	$2616.862 + 0.0i$
9	$3188.356 + 0.0i$	$3092.715 + 0.0i$
10	$3188.363 + 0.0i$	$3092.722 + 0.0i$

The eigenfunctions for fundamental eigenvalue ($i = 1$) of the α-spectral problem without delayed neutron are shown in Fig. 5. Due to the fact that the reactor state is close to critical ($k = k_1 \approx 0.97935$), the fundamental eigenfunctions of the λ-spectral problem are close to the fundamental eigenfunctions of the α-spectral problem. The eigenfunctions $\phi_1^{(i)}, i = 2, 3, 4, 5$ are shown in Fig. 6, Fig. 7.

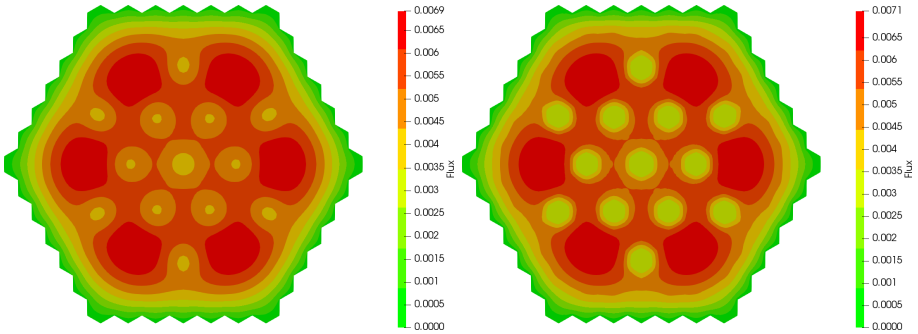

Figure 5: Eigenfunctions $\phi_1^{(1)}$, $\phi_2^{(1)}$ using SP_3 model.

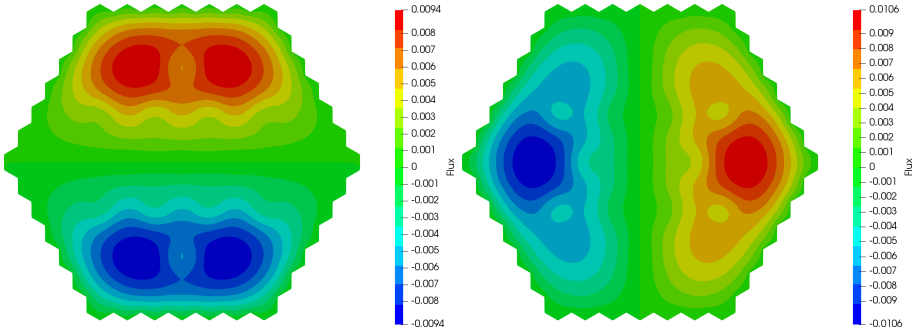

Figure 6: Eigenfunctions $\phi_1^{(2)}$, $\phi_1^{(3)}$ using SP_3 model.

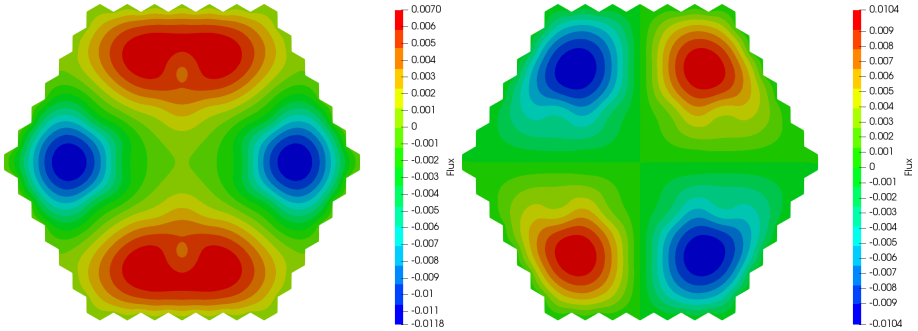

Figure 7: Eigenfunctions $\phi_1^{(4)}$, $\phi_1^{(5)}$ using SP_3 model.

4.1.3. Solution of α-spectral problem with delayed neutrons

As a reference solution for both the diffusion and transport SP_3 models, we used the solutions obtained using very fine mesh ($p = 3, n = 96$). The α-

spectral problem results with delayed neutrons using the different meshes and finite element orders are shown in Table 6. Compared with the previous case without delayed neutrons, these data demonstrate the similar convergence of the computed eigenvalues.

Table 6: The α-eigenvalues.

n	p	α_{dif}	Δ_{dif}	α_{sp_3}	Δ_{sp_3}
6	1	0.06465	0.00264	0.06410	0.00295
	2	0.06232	0.00031	0.06153	0.00035
	3	0.06206	0.00005	0.06122	0.00007
24	1	0.06296	0.00095	0.06224	0.00109
	2	0.06207	0.00005	0.06123	0.00008
	3	0.06202	0.00001	0.06116	0.00001
96	1	0.06228	0.00027	0.06147	0.00032
	2	0.06202	0.00001	0.06116	0.00001
	3	0.06201	–	0.06115	–
Ref.		0.06201		0.06115	

Table 7: The eigenvalues $\alpha_i = \lambda_i^{(\alpha)}$ for $p = 3, n = 96$.

i	Diffusion	SP_3
1	$0.06201 + 0.0i$	$0.06115 + 0.0i$
2	$0.06837 + 0.0i$	$0.06796 + 0.0i$
3	$0.06837 + 0.0i$	$0.06796 + 0.0i$
4	$0.07279 + 0.0i$	$0.07258 + 0.0i$
5	$0.07279 + 0.0i$	$0.07258 + 0.0i$
6	$0.07446 + 0.0i$	$0.07430 + 0.0i$
7	$0.07547 + 0.0i$	$0.07536 + 0.0i$
8	$0.07662 + 0.0i$	$0.07652 + 0.0i$
9	$0.07717 + 0.0i$	$0.07709 + 0.0i$
10	$0.07721 + 0.0i$	$0.07711 + 0.0i$

The first 10 spectral problem eigenvalues are shown in Table 7. Due to the contribution of delayed neutrons, the fundamental eigenvalue is much smaller compared with the case without delayed neutrons.

The eigenfunctions for fundamental eigenvalue ($i = 1$) of the α-spectral problem with delayed neutron are shown in Fig. 8. The eigenfunctions $\phi_1^{(i)}, i = 2, 3, 4, 5$ are shown in Fig. 9, Fig. 10. The eigenfunctions of the problems without and with delayed neutrons are close to each other in topology.

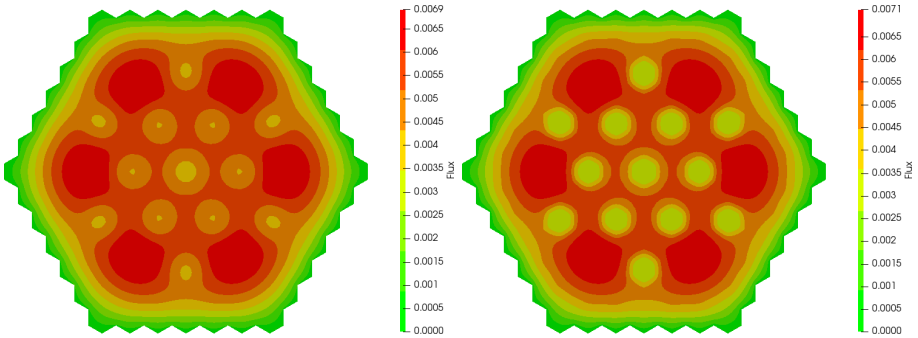

Figure 8: Eigenfunctions $\phi_1^{(1)}$, $\phi_2^{(1)}$.

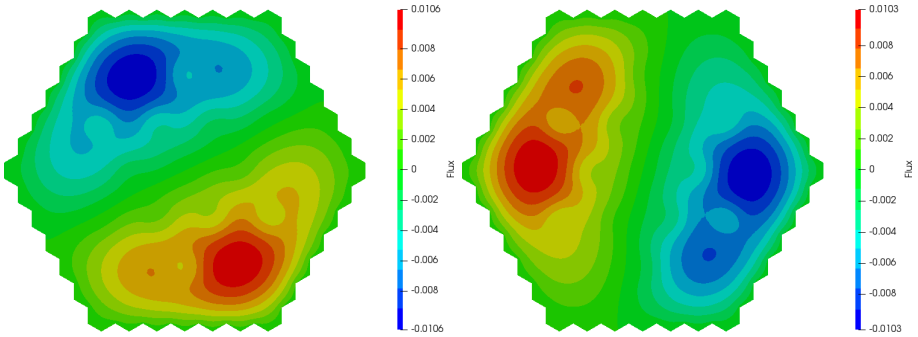

Figure 9: Eigenfunctions $\phi_1^{(2)}$, $\phi_1^{(3)}$.

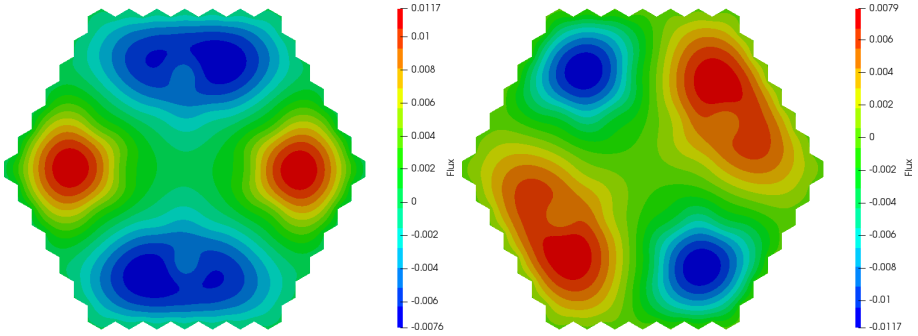

Figure 10: Eigenfunctions $\phi_1^{(4)}$, $\phi_1^{(5)}$.

4.2. IAEA-2D with reflector

This test differs from the previous one only additional external row of reflector assemblies (material 4, see Table 1).

4.2.1. Solution of Lambda Modes spectral problem

As a reference solution for the diffusion model, we used the previous results (Avvakumov et al., 2015); for the SP_3 model — the solution obtained using the MCNP4C code (Bahabadi et al., 2016). As well as in the previous benchmark calculations, the maximum difference in assembly power between two models is about 2 percent for the rodded assemblies (material 3, see Fig. 2).

The comparison of the calculated effective multiplication factors is shown in Table 8. The results of the first 10 eigenvalues for $p = 3, n = 96$ are presented in Table 9. The power distributions and calculation errors for $p = 2, n = 24$ using the diffusion model are shown in Fig 11 and for $p = 3, n = 96$ using the SP_3 model are shown Fig 12.

Table 8: The effective multiplication factor.

n	p	k_{dif}	Δ_{dif}, pcm	δ_{dif}	k_{sp_3}	Δ_{sp_3}, pcm	δ_{sp_3}
	1	1.01041	490	13.29	1.01159	536	14.14
6	2	1.00623	72	1.88	1.00711	88	2.19
	3	1.00558	7	0.22	1.00636	13	0.35
	1	1.00699	148	4.54	1.00792	169	4.96
24	2	1.00561	10	0.30	1.00640	17	0.42
	3	1.00551	0	0.02	1.00626	3	0.17
	1	1.00591	36	1.28	1.00671	48	1.42
96	2	1.00552	1	0.04	1.00626	3	0.18
	3	1.00551	0	0.01	1.00625	2	0.18
Ref.		1.00551			1.00623		

Table 9: The eigenvalues $k_i = 1/\lambda_i^{(k)}$ for $p = 3, n = 96$.

i	Diffusion	SP_3
1	$1.005510 + 0.0i$	$1.006245 + 0.0i$
2	$0.996490 + 0.0i$	$0.997254 + 0.0i$
3	$0.996490 + 0.0i$	$0.997254 + 0.0i$
4	$0.976791 + 0.0i$	$0.977759 + 0.0i$
5	$0.976791 + 0.0i$	$0.977759 + 0.0i$
6	$0.958684 + 0.0i$	$0.959895 + 0.0i$
7	$0.928980 + 0.0i$	$0.930969 + 0.0i$
8	$0.924186 + 0.0i$	$0.925931 + 0.0i$
9	$0.904788 + 0.0i$	$0.907349 + 0.0i$
10	$0.904788 + 0.0i$	$0.907349 + 0.0i$

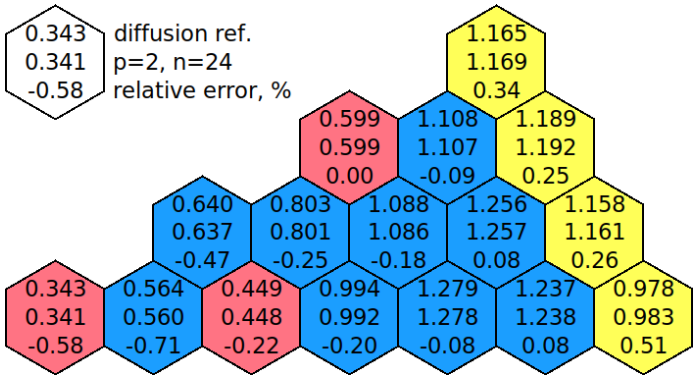

Figure 11: Power and error distributions using the diffusion model.

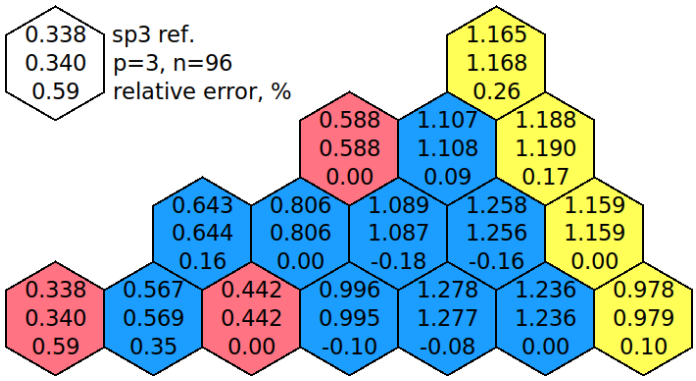

Figure 12: Power and error distributions using the SP_3 model.

4.2.2. Solution of α-spectral problem without delayed neutrons

As a reference solution, we use the fine mesh solutions obtained using the diffusion or transport SP_3 model ($p = 3, n = 96$). The α-spectral problem results are shown in Table 10.

Table 10: The α-eigenvalues.

n	p	α_{dif}	Δ_{dif}	α_{sp_3}	Δ_{sp_3}
6	1	-184.95	84.14	-205.92	91.32
	2	-113.58	12.77	-130.02	15.42
	3	-101.98	1.17	-116.72	2.12
24	1	-126.66	25.85	-143.85	29.25
	2	-102.58	1.77	-117.31	2.71
	3	-100.88	0.07	-114.83	0.23
96	1	-107.82	7.01	-122.84	8.24
	2	-100.97	0.16	-114.94	0.34
	3	-100.81	–	-114.60	–
Ref.		-100.81		-114.60	

According to (11), the prompt neutron lifetime $l_{pr} \approx 5.4 \cdot 10^{-5}$ sec for both the diffusion and SP_3 models.

The results of the first 10 eigenvalues for $p = 3, n = 96$ are presented in Table 9. As before, the eigenvalues are well separated. In this example, the fundamental eigenvalue is negative and therefore the main harmonic will increase, while all others will attenuate.

The eigenfunctions for fundamental eigenvalue ($i = 1$) of the α-spectral problem without delayed neutrons are shown in Fig. 13. Due to the fact that a state of the reactor is close to critical ($k = k_1 \approx 1.00625$), the fundamental eigenfunctions of the λ-spectral problem are close to the fundamental eigenfunc-

Table 11: The eigenvalues $\alpha_i = \lambda_i^{(\alpha)}$ for $p = 3, n = 96$.

i	Diffusion	SP_3
1	$-100.81 + 0.0i$	$-114.60 + 0.0i$
2	$62.93 + 0.0i$	$49.42 + 0.0i$
3	$62.93 + 0.0i$	$49.42 + 0.0i$
4	$405.31 + 0.0i$	$390.15 + 0.0i$
5	$405.31 + 0.0i$	$390.15 + 0.0i$
6	$710.64 + 0.0i$	$693.47 + 0.0i$
7	$1141.43 + 0.0i$	$1118.67 + 0.0i$
8	$1469.68 + 0.0i$	$1438.31 + 0.0i$
9	$1494.37 + 0.0i$	$1468.54 + 0.0i$
10	$1494.37 + 0.0i$	$1468.54 + 0.0i$

tions of the α-spectral problem. The eigenfunctions $\phi_1^{(i)}, i = 2, 3, 4, 5$ are shown in Fig. 14, Fig. 15.

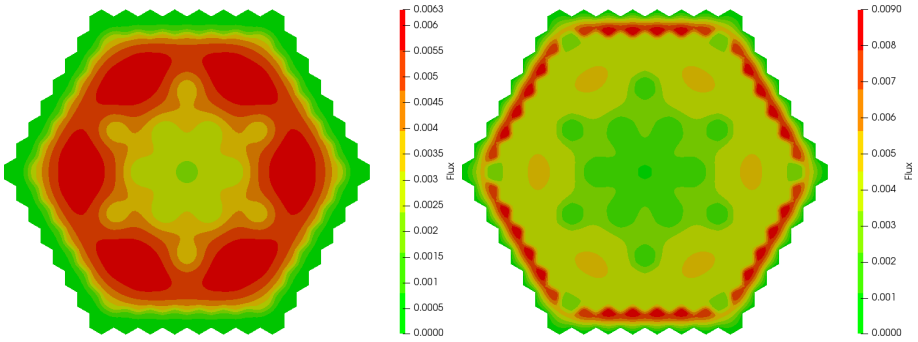

Figure 13: Eigenfuncions $\phi_1^{(1)}$, $\phi_2^{(1)}$.

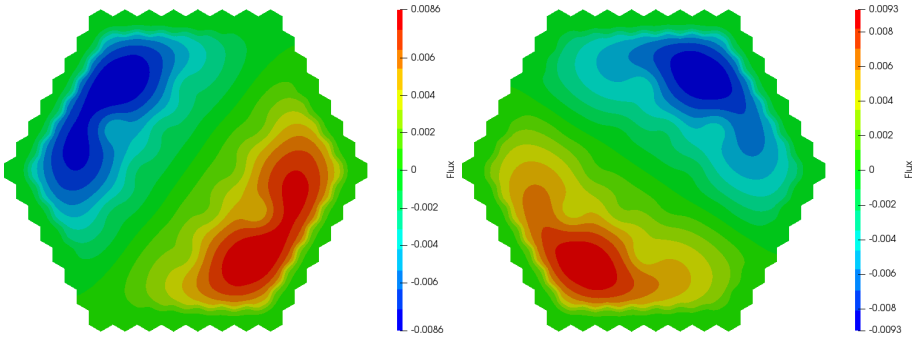

Figure 14: Eigenfuncions $\phi_1^{(2)}$, $\phi_1^{(3)}$.

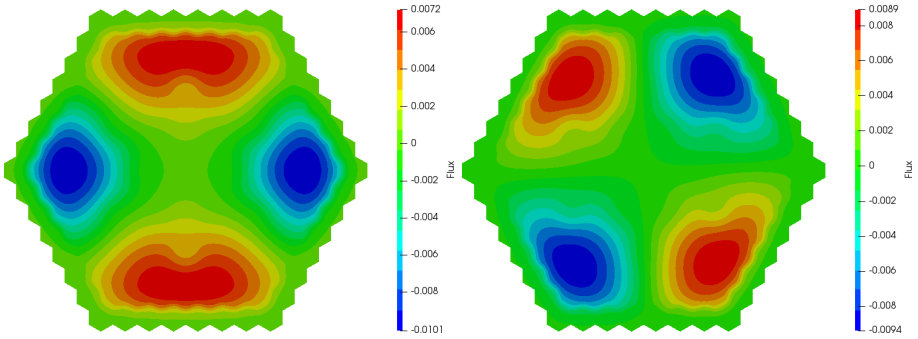

Figure 15: Eigenfuncions $\phi_1^{(4)}$, $\phi_1^{(5)}$.

4.2.3. Solution of α-spectral problem with delayed neutrons

As a reference solution, we use the fine mesh solutions obtained using the diffusion or transport SP_3 model ($p = 3, n = 96$). The α-spectral problem results are shown in Table 12.

The calculation results for the first 10 eigenvalues are shown in Table 13. Due to the contribution of delayed neutrons, the fundamental eigenvalue is much smaller than in the case without delayed neutrons. Again the fundamental eigenvalue is negative and therefore the main harmonic will increase, while all others will attenuate.

The eigenfunctions for fundamental eigenvalue ($i = 1$) of the α-spectral problem with delayed neutrons are presented in Fig. 16. The eigenfunctions $\phi_1^{(i)}, i = 2, 3, 4, 5$ are shown in Fig. 17, Fig. 18. The eigenfunctions of the problems without and with delayed neutrons are close to each other in topology.

Table 12: The α-eigenvalues.

n	p	α_{dif}	Δ_{dif}	α_{sp_3}	Δ_{sp_3}
	1	-68.2268	67.8084	-88.9461	87.6086
6	2	-1.2810	0.8626	-11.1554	9.8179
	3	-0.4506	0.0322	-1.8063	0.4688
	1	-9.0267	8.6083	-25.1658	23.8283
24	2	-0.4686	0.0502	-1.9832	0.6457
	3	-0.4202	0.0018	-1.3787	0.0412
	1	-0.7018	0.2834	-4.9794	3.6419
96	2	-0.4225	0.0041	-1.3994	0.0619
	3	-0.4184	–	-1.3375	–
Ref.		-0.4184		-1.3375	

Table 13: The eigenvalues $\alpha_i = \lambda_i^{(\alpha)}$ for $p = 3, n = 96$.

i	Diffusion	SP_3
1	$-0.4184 + 0.0i$	$-1.3375 + 0.0i$
2	$0.0281 + 0.0i$	$0.0238 + 0.0i$
3	$0.0281 + 0.0i$	$0.0238 + 0.0i$
4	$0.0628 + 0.0i$	$0.0622 + 0.0i$
5	$0.0628 + 0.0i$	$0.0622 + 0.0i$
6	$0.0695 + 0.0i$	$0.0692 + 0.0i$
7	$0.0737 + 0.0i$	$0.0736 + 0.0i$
8	$0.0741 + 0.0i$	$0.0740 + 0.0i$
9	$0.0754 + 0.0i$	$0.0752 + 0.0i$
10	$0.0763 + 0.0i$	$0.0762 + 0.0i$

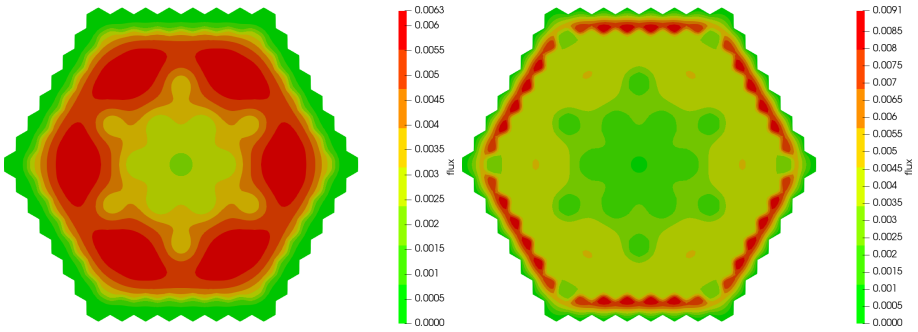

Figure 16: Eigenfunctions $\phi_1^{(1)}$, $\phi_2^{(1)}$.

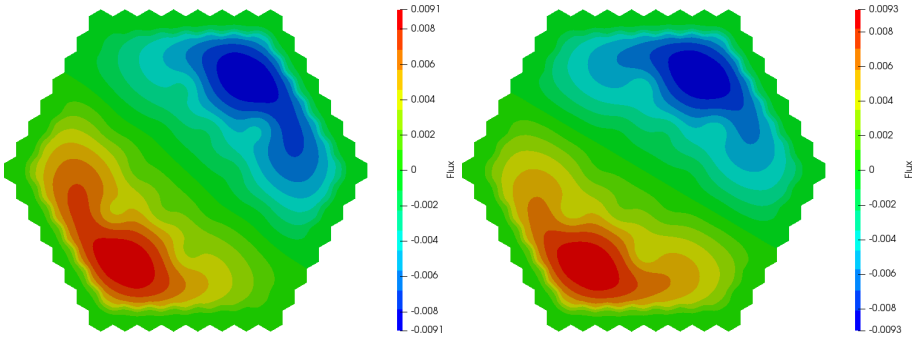

Figure 17: Eigenfunctions $\phi_1^{(2)}$, $\phi_1^{(3)}$.

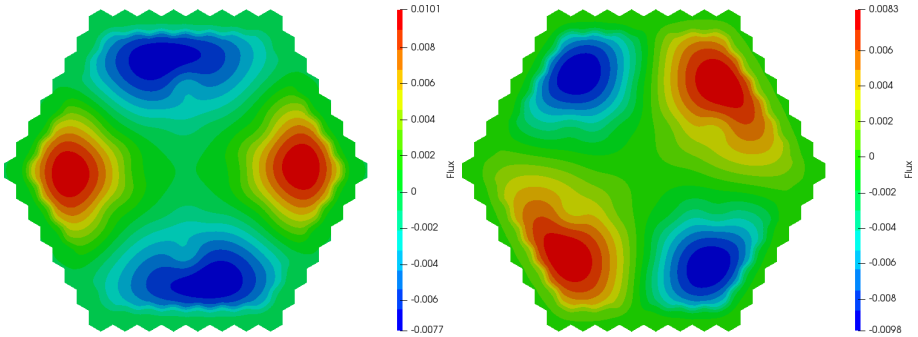

Figure 18: Eigenfunctions $\phi_1^{(4)}$, $\phi_1^{(5)}$.

4.3. Azimutally non-symmetric test IAEA-2D with reflector

To investigate azimutally non-symmetric geometry effects on the eigenfunction behaviour, we replaced two unrodded assemblies in the north-east part of the core by rodded ones (material 3, see Fig. 19).

4.3.1. Solution of Lambda Modes spectral problem

As a reference solution for both the diffusion and transport SP_3 models, we used the solutions obtained using very fine mesh ($p = 3, n = 96$). The effective multiplication factors are shown in Table 14. The results of the first 10 eigenvalues for $p = 3, n = 96$ are presented in Table 15.

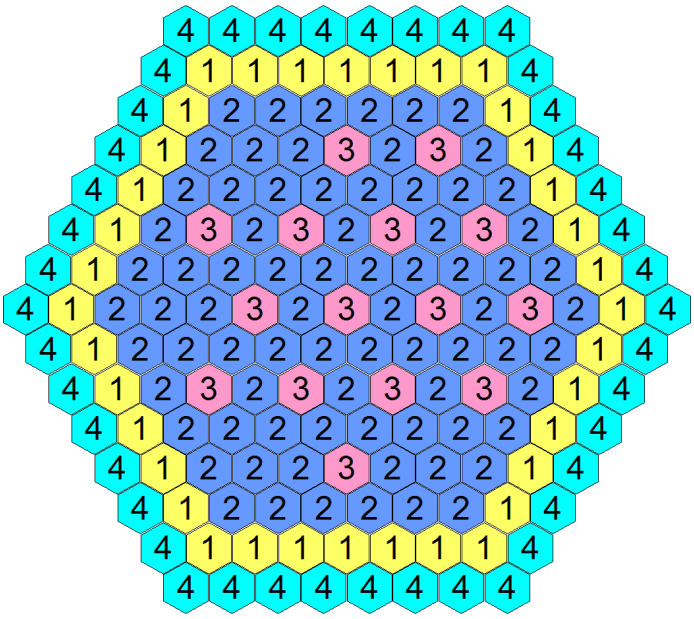

Figure 19: Geometrcial model of the non-symmetric test IAEA-2D.

Table 14: The effective multiplication factor.

n	p	k_{dif}	Δ_{dif}	k_{sp_3}	Δ_{sp_3}
	1	1.00809	509	1.009309	555.8
6	2	1.00374	74	1.004655	90.4
	3	1.00306	6	1.003875	12.4
	1	1.00454	154	1.005501	175.0
24	2	1.00310	10	1.003910	15.9
	3	1.00300	0	1.003764	1.3
	1	1.00341	41	1.004241	49.0
96	2	1.00300	0	1.003771	2.0
	3	1.00300	–	1.003751	–
Ref.		1.00300		1.003751	

Table 15: The eigenvalues $k_i = 1/\lambda_i^{(k)}$ for $p = 3, n = 96$.

i	diffusion	SP_3
1	$1.002996 + 0.0i$	$1.003751 + 0.0i$
2	$0.994571 + 0.0i$	$0.995365 + 0.0i$
3	$0.986297 + 0.0i$	$0.987243 + 0.0i$
4	$0.970315 + 0.0i$	$0.971407 + 0.0i$
5	$0.968980 + 0.0i$	$0.970207 + 0.0i$
6	$0.945551 + 0.0i$	$0.947166 + 0.0i$
7	$0.928439 + 0.0i$	$0.930441 + 0.0i$
8	$0.923863 + 0.0i$	$0.925611 + 0.0i$
9	$0.903265 + 0.0i$	$0.905868 + 0.0i$
10	$0.901593 + 0.0i$	$0.904253 + 0.0i$

4.3.2. Solution of α-spectral problem without delayed neutrons

As a reference solution for both the diffusion and SP_3 models, we used the solutions obtained using very fine mesh ($p = 3, n = 96$). The α-spectral problem results are shown in Table 16. The results of the first 10 eigenvalues for $p = 3, n = 96$ are presented in Table 17.

Table 16: The α-eigenvalues.

n	p	α_{dif}	Δ_{dif}	α_{sp_3}	Δ_{sp_3}
	1	−143.12	88.55	−164.63	96.08
6	2	−67.99	13.42	−84.75	16.20
	3	−55.82	1.25	−70.78	2.23
	1	−81.93	27.36	−99.47	30.92
24	2	−56.45	1.88	−71.41	2.86
	3	−54.65	0.08	−68.80	0.25
	1	−62.00	7.43	−77.28	8.73
96	2	−54.74	0.17	−68.91	0.36
	3	−54.57	–	−68.55	–
Ref.		−54.57		−68.55	

According to (11), the prompt neutron lifetime $l_{pr} \approx 5.5 \cdot 10^{-5}$ sec for both the diffusion and SP_3 models. Thus, for the non-symmetric test we obtained similar neutronic properties compared with the symmetric test.

Let's consider changes in the eigenfunctions due to the rodded assembly insertion. The eigenfunctions for fundamental eigenvalue ($i = 1$) of the α-spectral problem without delayed neutrons are shown in Fig. 20. The eigenfunctions $\phi_1^{(i)}, i = 2, 3, 4, 5$ are shown in Fig. 21, Fig. 22. As can be seen from Fig. 20 to Fig. 22, the overal structure of the eigenfunctions is preserved taking into account the neutron flux perturbations.

Table 17: The eigenvalues $\alpha_i = \lambda_i^{(\alpha)}$ for $p = 3, n = 96$.

i	Diffusion	SP_3
1	-54.57 + 0.0i	-68.55 + 0.0i
2	97.07 + 0.0i	83.18 + 0.0i
3	242.22 + 0.0i	226.42 + 0.0i
4	513.07 + 0.0i	496.61 + 0.0i
5	530.98 + 0.0i	512.74 + 0.0i
6	898.88 + 0.0i	878.37 + 0.0i
7	1148.46 + 0.0i	1125.66 + 0.0i
8	1481.13 + 0.0i	1449.58 + 0.0i
9	1512.16 + 0.0i	1486.05 + 0.0i
10	1527.83 + 0.0i	1501.83 + 0.0i

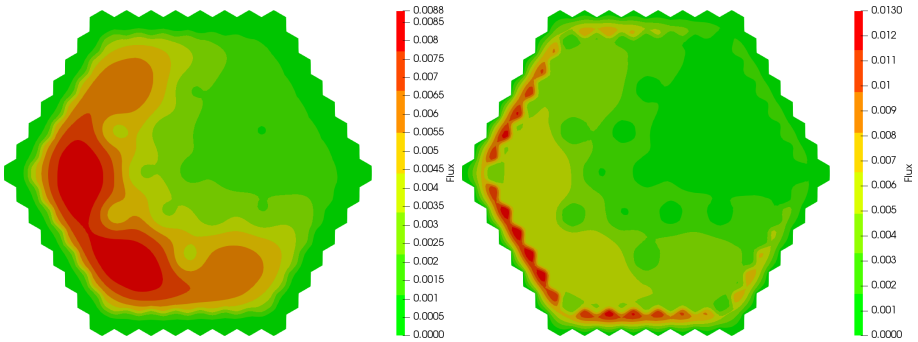

Figure 20: Eigenfunctions $\phi_1^{(1)}$, $\phi_2^{(1)}$.

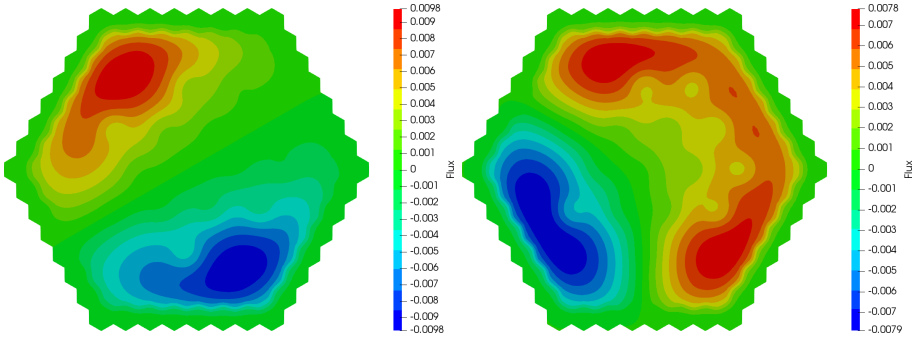

Figure 21: Eigenfunctions $\phi_1^{(2)}$, $\phi_1^{(3)}$.

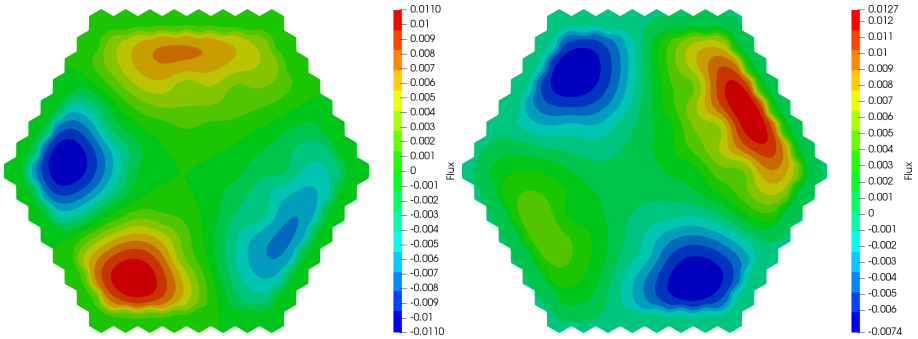

Figure 22: Eigenfunctions $\phi_1^{(4)}$, $\phi_1^{(5)}$.

4.4. HWR test problem

This benchmark is a model of large heavy-water reactor HWR (Chao and Shatilla, 1995). The geometry of the HWR test is presented in Fig. 23. Fuel assemblis (1, 2, 3 and 6 in Fig. 23) located in the central part of the core, are surrouded by the target zone and reflector layer (7 and 9 in Fig. 23). There are two types of rodded assemblies (4 and 8). The assembly size is equal to 17.78 cm.

Diffusion constants are given in Table 18. The following delayed neutrons parameters are used: one group of delayed neutrons with effective fraction $\beta_1 = 6.5 \cdot 10^{-3}$ and decay constant $\lambda_1 = 0.08$ s^{-1}. Neutron velocity $v_1 = 1.25 \cdot 10^7$ cm/s and $v_2 = 2.5 \cdot 10^5$ cm/s.

4.4.1. Solution of Lambda Modes spectral problem

Table 19: The effective multiplication factor.

n	p	k_{dif}	Δ_{dif}, pcm	δ_{dif}	k_{sp_3}	Δ_{sp_3}, pcm	δ_{dif}
	1	0.991985	2.0	1.16	0.992178	5.0	0.80
6	2	0.991989	2.4	0.31	0.992166	3.8	0.24
	3	0.991964	0.1	0.08	0.992132	0.4	0.07
	1	0.991983	1.8	0.05	0.992165	3.7	0.08
24	2	0.991965	0.0	0.01	0.992133	0.5	0.01
	3	0.991963	0.2	0.01	0.992128	0.0	0.00
	1	0.991969	0.4	0.08	0.992140	1.2	0.01
96	2	0.991963	0.2	0.02	0.992129	0.1	0.00
	3	0.991963	0.2	0.01	0.992128	–	–
Ref.		0.991965			0.992128		

As a reference solution for the diffusion model, we used the results obtained by (Chao and Shatilla, 1995); for the SP_3 model — the solution obtained using

Table 18: Diffusion constants for HWR test.

Material	Group	D, cm	Σ_r, cm^{-1}	$\Sigma_{1\to2}$, cm^{-1}	$\nu\Sigma_f$, cm^{-1}
1	1	1.38250058	1.1105805e-2	8.16457e-3	2.26216e-3
	2	0.89752185	2.2306487e-2		2.30623e-2
2	1	1.38255219	1.1174585e-2	8.22378e-3	2.22750e-3
	2	0.89749043	2.2387609e-2		2.26849e-2
3	1	1.37441741	1.0620368e-2	8.08816e-3	2.14281e-3
	2	0.88836771	1.6946527e-2		2.04887e-2
4	1	1.31197955	1.2687953e-2	1.23115e-2	0.0
	2	0.87991376	5.2900925e-2		0.0
6	1	1.38138909	1.056312e-2	7.76568e-3	2.39469e-3
	2	0.90367052	2.190298e-2		2.66211e-2
7	1	1.30599110	1.1731321e-2	1.10975e-2	0.0
	2	0.83725587	4.3330365e-3		0.0
8	1	1.29192957	1.1915316e-2	1.15582e-2	0.0
	2	0.81934103	3.0056488e-4		0.0
9	1	1.06509884	2.8346221e-2	2.61980e-2	0.0
	2	0.32282849	3.3348874e-2		0.0

very fine mesh ($p = 3, n = 96$).

The effective multiplication factors for the HWR test are shown in Table 19.

The results of the first 10 eigenvalues for $p = 3, n = 96$ are presented in Table 20. The eigenvalues $k_2, k_3, k_4, k_5, k_9, k_{10}$ of the λ-spectral problem are the complex values with small imaginary parts, and the eigenvalues k_1, k_6, k_7, k_8 are the real values.

4.4.2. Solution of α-spectral problem without delayed neutrons

As a reference solution for the diffusion and SP_3 models we use the solutions obtained using very fine mesh ($p = 3, n = 96$).

The α-spectral problem results at different computational parameters are shown in Table 21. The results of the first 10 eigenvalues for $p = 3, n = 96$ are presented in Table 22. The eigenvalues are well separated. The eigenvalues $\alpha_2, \alpha_3, \alpha_4, \alpha_5, \alpha_9, \alpha_{10}$ of the α-spectral problem, like for the λ-spectral problem, are the complex values with small imaginary parts, and the eigenvalues $\alpha_1, \alpha_6, \alpha_7, \alpha_8$ are the real values.

According to (11), the prompt neutron lifetime $l_{pr} \approx 1.9 \cdot 10^{-4}$ sec for both the diffusion and SP_3 models. This is a typical value of the HWR prompt neutron lifetime (more than 20 times less compared with the considered light water tests IAEA-2D).

The eigenfunctions for fundamental eigenvalue ($n = 1$) of the α-spectral problem are shown in Fig. 24. The real part of the eigenfunctions $\phi_1^{(n)}$, $n = 2, 3, 4, 5$ is shown in Fig. 25. Fig. 26 shows the imaginary part of these eigenfunc-

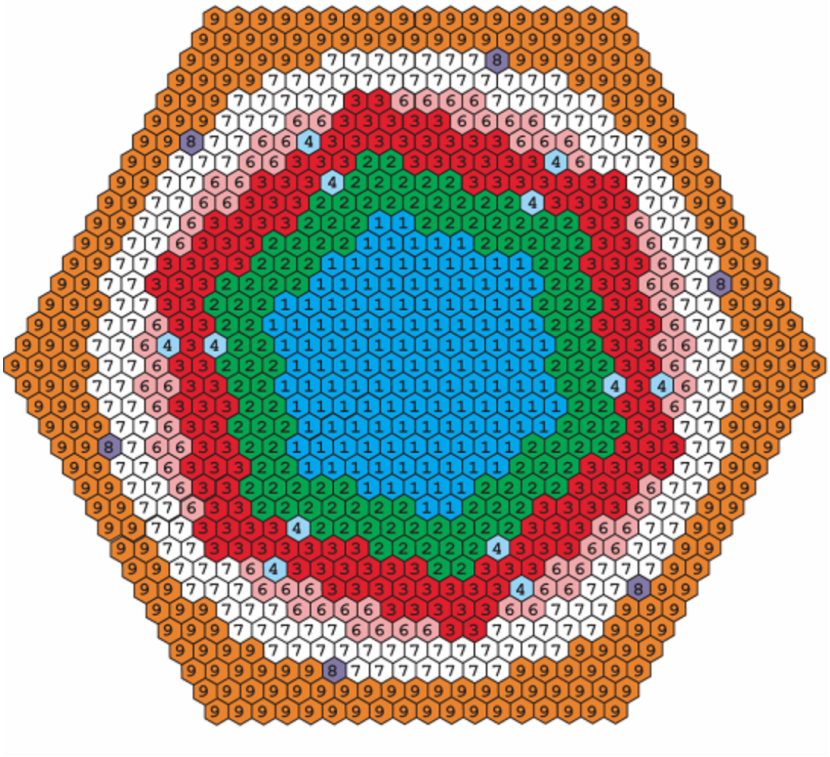

Figure 23: Geometrcial model of the HWR test.

tions. The eigenfunctions of the λ-spectral and α-spectral problems are close to each other in topology.

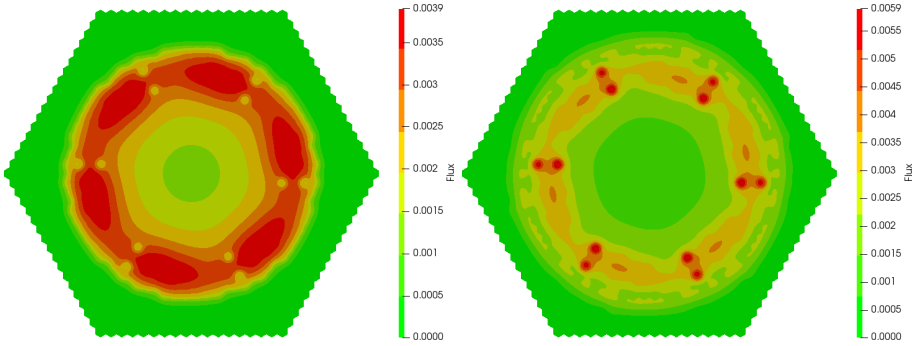

Figure 24: The eigenfunctions $\phi_1^{(1)}$ (left) and $\phi_2^{(1)}$ (right).

Table 20: The eigenvalues $k_i = 1/\lambda_i^{(k)}$ for $p = 3, n = 96$.

i	diffusion	SP_3
1	$0.991963 + 0.0i$	$0.992128 + 0.0i$
2	$0.983594 + 1.1645\text{e-}05i$	$0.983793 + 1.2072\text{e-}05i$
3	$0.983594 - 1.1645\text{e-}05i$	$0.983793 - 1.2072\text{e-}05i$
4	$0.964240 + 2.1564\text{e-}05i$	$0.964523 + 2.2337\text{e-}05i$
5	$0.964240 - 2.1564\text{e-}05i$	$0.964523 - 2.2337\text{e-}05i$
6	$0.943290 + 0.0i$	$0.943733 + 0.0i$
7	$0.923872 + 0.0i$	$0.924257 + 0.0i$
8	$0.918657 + 0.0i$	$0.918798 + 0.0i$
9	$0.895682 + 3.5570\text{e-}05i$	$0.896317 + 3.6750\text{e-}05i$
10	$0.895682 - 3.5570\text{e-}05i$	$0.896317 + 3.6750\text{e-}05i$

Table 21: The α-eigenvalues.

n	p	α_{dif}	Δ_{dif}	α_{sp_3}	Δ_{sp_3}
	1	42.281	0.018	41.246	0.134
6	2	42.135	0.128	41.190	0.190
	3	42.259	0.004	41.362	0.018
	1	42.196	0.067	41.228	0.152
24	2	42.253	0.010	41.354	0.026
	3	42.263	0.000	41.379	0.001
	1	42.241	0.022	41.330	0.050
96	2	42.262	0.001	41.377	0.003
	3	42.263	–	41.380	–
Ref.		42.263		41.380	

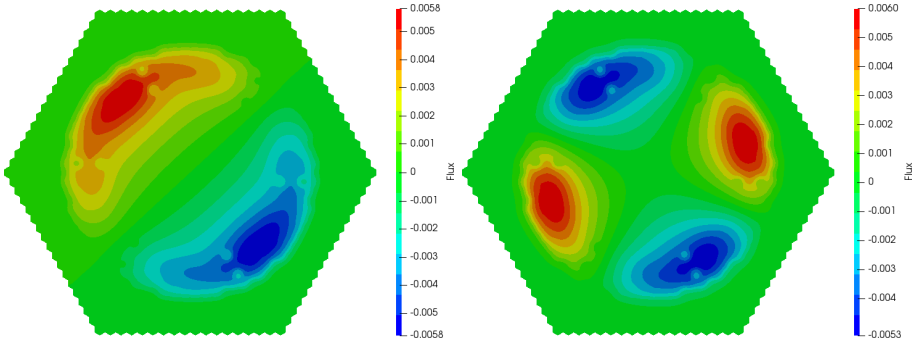

Figure 25: Real part of eigenfunctions $\phi_1^{(2)}$, $\phi_1^{(3)}$ (left) and $\phi_1^{(4)}$, $\phi_1^{(5)}$ (right).

Table 22: The eigenvalues $\alpha_i = \lambda_i^{(\alpha)}$ for $p = 3, n = 96$.

i	Diffusion	SP_3
1	$42.263 + 0.0i$	$41.380 + 0.0i$
2	$84.867 - 0.06130i$	$83.821 - 0.06358i$
3	$84.867 + 0.06130i$	$83.821 + 0.06358i$
4	$182.914 - 0.11367i$	$181.471 - 0.11805i$
5	$182.914 + 0.11367i$	$181.471 + 0.11805i$
6	$293.017 + 0.0i$	$290.940 + 0.0i$
7	$371.528 + 0.0i$	$369.374 + 0.0i$
8	$515.465 - 0.16397i$	$512.337 - 0.17197i$
9	$515.465 + 0.16397i$	$512.337 + 0.17197i$
10	$518.670 + 0.0i$	$517.975 + 0.0i$

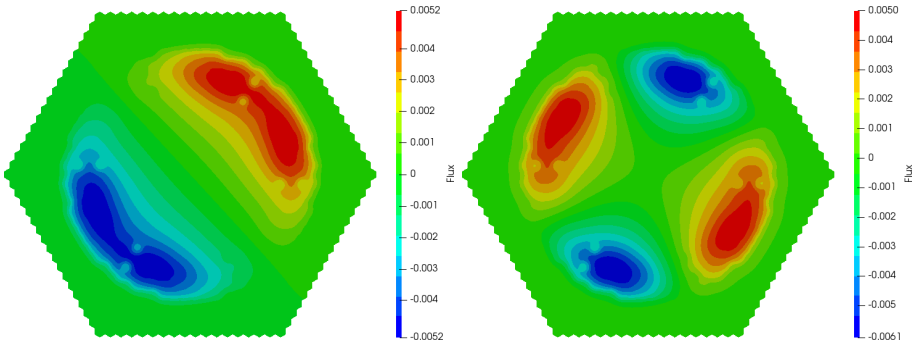

Figure 26: Imaginary part of eigenfunctions $\phi_1^{(2)}$, $-\phi_1^{(3)}$ (left) and $\phi_1^{(4)}$, $-\phi_1^{(5)}$ (right).

4.4.3. Solution of α-spectral problem with delayed neutrons

As a reference solution for the diffusion and SP_3 models we use the solutions obtained using very fine mesh ($p = 3, n = 96$).

The α-spectral problem results are shown in Table 23. Due to the contribution of delayed neutrons, the fundamental eigenvalue is much smaller than in the case without delayed neutrons. The results of the first 10 eigenvalues for $p = 3, n = 96$ is shown in Table 24. The eigenvalues α_2, α_3, α_4, α_5, α_9, α_{10} of the α-spectral problem, like as before, are the complex values with small imaginary parts, and the eigenvalues α_1, α_6, α_7, α_8 are the real values.

Table 23: The α-eigenvalues.

n	p	α_{dif}	Δ_{dif}	α_{sp_3}	Δ_{sp_3}
	1	0.04431	0.00006	0.04383	0.00012
6	2	0.04430	0.00007	0.04386	0.00009
	3	0.04437	0.00000	0.04394	0.00001
	1	0.04432	0.00005	0.04386	0.00009
24	2	0.04436	0.00001	0.04394	0.00001
	3	0.04437	0.00000	0.04395	0.00000
	1	0.04435	0.00002	0.04392	0.00003
96	2	0.04437	0.00000	0.04395	0.00000
	3	0.04437	–	0.04395	–
Ref.		0.04437		0.04395	

Table 24: The eigenvalues $\alpha_i = \lambda_i^{(\alpha)}$ for $p = 3, n = 96$.

i	Diffusion	SP_3
1	0.04437 + 0.0i	0.04395 + 0.0i
2	0.05755 − 1.15549e-05i	0.05735 − 1.22333e-05i
3	0.05755 + 1.15549e-05i	0.05735 + 1.22333e-05i
4	0.06807 − 6.35264e-06i	0.06798 − 6.66947e-06i
5	0.06807 + 6.35264e-06i	0.06798 + 6.66947e-06i
6	0.07219 + 0.0i	0.07213 + 0.0i
7	0.07415 + 0.0i	0.07412 + 0.0i
8	0.07453 + 0.0i	0.07452 + 0.0i
9	0.07577 − 1.52484e-06i	0.07574 − 1.60360e-06i
10	0.07577 + 1.52484e-06i	0.07574 + 1.60360e-06i

Conclusion

Simulation of reactor dynamic processes is basically considered on the basis of multigroup diffusion approximation of the neutron transport equation. To improve the calculation accuracy for some situations of interest, including pin-by-pin calculations, the SP_3 approximation was adopted in different whole-core diffusion codes as an improved option compared with the diffusion approximation. In this regard, it will be very useful to compare the spectral parameters, calculated by both the diffusion and SP_3 options using the finite element method.

Solution of the λ- and α-spectral problems has been tested for the IAEA-2D and HWR reactor benchmark tests. The classical Lagrange finite elements are used for the spatial approximation. Accuracy control is performed using condensed grids. Spectral problems are solved numerically using well-developed

free software SLEPc and using GMSH as a generic mesh generator.

It was found noticeable differences in α-eigenvalues problems taking into account delayed neutrons. Of particular interest is the problem associated with appearance of complex eigenvalues and eigenfunctions. It was found that this tendency occurs for both the diffusion and SP_3 solutions of the HWR reactor test. On the contrary, solutions of the IAEA-2D benchmark test showed the absence of complex eigenvalues and eigenfunctions, even in a skew-symmetric variant of the benchmark.

Acknowledgements

This work was supported by the grant of the Russian Federation Government (# 14.Y26.31.0013) and by the Russian Foundation for Basic Research (# 18-31-00315).

Avvakumov, A.V., Strizhov, V.F., Vabishchevich, P.N., Vasilev, A.O., 2017. Spectral properties of dynamic processes in a nuclear reactor. Annals of Nuclear Energy 99, 68–79.

Avvakumov, A.V., Vabishchevich, P.N., Vasilev, A.O., 2014. Metod konechnyh ehlementov dlya uravneniya diffuzii nejtronov v geksagonal'noj geometrii. Vestnik of North-Eastern Federal University 11, 7–18.

Avvakumov, A.V., Vasilev, A.O., Zakharov, P.E., 2015. Programmnaya realizaciya metoda konechnyh ehlementov dlya uravneniya diffuzii nejtronov. Vestnik of North-Eastern Federal University .

Azmy, Y., Sartori, E., 2010. Nuclear computational science: a century in review. Springer.

Bahabadi, M.H., Pazirandeh, A., Mitra, A., 2016. Analytic function expansion nodal (AFEN) method for solving multigroup neutron simplified P_3 (SP_3) equations in hexagonal-z geometry. Annals of Nuclear Energy 98, 74–80.

Beckert, C., Grundmann, U., 2008. Development and verification of a nodal approach for solving the multigroup SP_3 equations. Annals of Nuclear Energy 35, 75–86.

Bell, G.I., Glasstone, S., 1970. Nuclear Reactor Theory. Van Nostrand Reinhold Company.

Brantley, P.S., Larsen, E.W., 2000. The simplified P_3 approximation. Nuclear Science and Engineering 134, 1–21.

Brenner, S.C., Scott, L.R., 2008. The mathematical theory of finite element methods. Springer.

Brewster, W.J., 2018. Development and Monte Carlo validation of a finite element reactor analysis framework. Masters Theses 7756, Missouri University of Science and Technology .

Chao, Y.A., Shatilla, Y.A., 1995. Conformal mapping and hexagonal nodal methods-II: Implementation in the ANC-H Code. Nuclear Science and Engineering 121, 210–225.

Downar, T., Xu, Y., Seker, V., Hudson, N., 2010. Theory manual for the PARCS kinetics core simulator module. Department of Nuclear Engineering and Radiological Sciences, University of Michigan .

Gelbard, E.M., 1960. Application of spherical harmonics method to reactor problems. Bettis Atomic Power Laboratory, West Mifflin, PA, Technical Report No. WAPD-BT-20 .

Gelbard, E.M., 1961. Simplified spherical harmonics equations and their use in shielding problems. Technical Report. Westinghouse Electric Corp. Bettis Atomic Power Lab., Pittsburgh.

Gelbard, E.M., 1962. Applications of the simplified spherical harmonics equations in spherical geometry. Technical Report. Westinghouse Electric Corp. Bettis Atomic Power Lab., Pittsburgh.

Ginestar, D., Miro, R., Verdu, G., Hennig, D., 2002. A transient modal analysis of a BWR instability event. Journal of Nuclear Science and Technology 39, 554–563.

Lawrence, R.D., 1986. Progress in nodal methods for the solution of the neutron diffusion and transport equations. Progress in Nuclear Energy 17, 271–301.

Logg, A., Mardal, K.A., Wells, G., 2012. Automated solution of differential equations by the finite element method: The FEniCS book. volume 84. Springer Science & Business Media.

McClarren, R.G., 2010. Theoretical aspects of the simplified P_N equations. Transport Theory and Statistical Physics 39, 73–109.

Quarteroni, A., Valli, A., 2008. Numerical approximation of partial differential equations. Springer.

Ryu, E.H., Joo, H.G., 2013. Finite element method solution of the simplified P_3 equations for general geometry applications. Annals of Nuclear Energy 56, 194–207.

Stacey, W.M., 2007. Nuclear Reactor Physics. Wiley.

Stewart, G.W., 2001. A Krylov–Schur algorithm for large eigenproblems. SIAM Journal on Matrix Analysis and Applications 23, 601–614.

Tada, K., Yamamoto, A., Yamane, Y., Kitamuray, Y., 2008. Applicability of the diffusion and simplified P_3 theories for pin-by-pin geometry of BWR. Journal of nuclear science and technology 45, 997–1008.

Verdu, G., Ginestar, D., 2014. Modal decomposition method for BWR stability analysis using alpha-modes. Annals of Nuclear Energy 67, 31–40.

Verdu, G., Ginestar, D., Roman, J., Vidal, V., 2010. 3D alpha modes of a nuclear power reactor. Journal of Nuclear Science and Technology 47, 501–514.